Comparison of Conformations of Thiocrown Ethers in Solid and Solution with Information on Conformational Flipping from Molecular Dynamics Calculations

Joyce C. Lockhart* and Nicholas P. Tomkinson
Dept. of Chemistry, Bedson Building, The University, Newcastle upon Tyne, NE1 7RU, UK

Studies intended to elucidate the conformational behaviour of simple thiocrown ethers are described. New NMR information on solution conformation is compared with available X-ray data, and with the patterns of conformational change seen when molecular dynamics (MD) simulations are performed on several of the molecules. Suitable protocols have been evaluated for the MD study and comments are made on the structural insight which MD simulations can provide for such molecules.

There has been conjecture about the role of the conformation of crown ethers and thioethers, in particular the importance of fluxionality, in the coordination processes for which such compounds are intended. It is relevant to know whether a particular conformational change takes place on a faster or slower timescale than the coordination, and whether it can take place on the coordinated ligand.[1] For many thiocrown ethers, where the free ligands have exodentate sulfurs, it has been supposed that a conformational switch to endodentate sulfurs is a prerequisite for complexation, and that an appropriate energy penalty is required.[2] In this paper we consider the conformational information on a series of simple thioether crowns, that already available from X-ray crystal structure information, new NMR solution studies which give an indication of the conformational mixture in solution, and the pattern of conformational changes obtained through molecular dynamics (MD) simulations. Comments on the significance of the comparisons are made.

The thiocrown macrocycles have come into great prominence recently, due to their ability to stabilise unusual oxidation states of the transition metals and coinage metals,[2,3] and the realisation of their potential as replacements for the unsavoury, toxic, air-sensitive phosphines as ligands in catalysts. There has been intense interest in the conformations of these ligands, since the size of the sulfur atom, and the tendency for torsion angles of C–C–S–C bonds to be *gauche* while those of S–C–C–S bonds are *anti* ensures that the conformations observed to date are very different from those of analogous crown ethers.[2] In the coordination processes for macrocycles, the conformation and fluxionality of the ligand are judged to be important. For example, a rigid structure has been proposed as an important requirement for high thermodynamic selectivity, Cram's preorganisation hypothesis,[4] although more recently Bell has suggested that for certain azacoronands this is not the case.[5] The small crown ether, 1,4,7-trithiacyclononane, which has the distinction, among simple thiocrown ethers, of having all its thioether donors pointing inwards (endodentate) in its crystal structure,[6] is said to be preorganised, and thus eminently suited to facial coordination to appropriate soft metal atoms. However, it is clear that in solution this structure is not rigid, but probably flipping rapidly betwen conformations, so as to render all its protons equivalent on the NMR timescale. Blom *et al.*[7] were unable to decide from electron diffraction data if the structure of this crown was the same in the gas phase as in the crystal. This paper reports a series of investigations on simple thiocrowns, for most of which there was available crystal structure data. The ^{1}H NMR spectra were determined and the coupling patterns analysed (using ^{13}C satellites where necessary). These reflect the proportion of *gauche* and *anti* S–C–C–S segments in the solution conformation. The behaviour of the molecules was also simulated using molecular mechanics and dynamics. Comparison of the structures determined by X-ray or electron diffraction methods and by NMR solution techniques with the simulated structures can be made. The compounds considered are **1**–**6**.

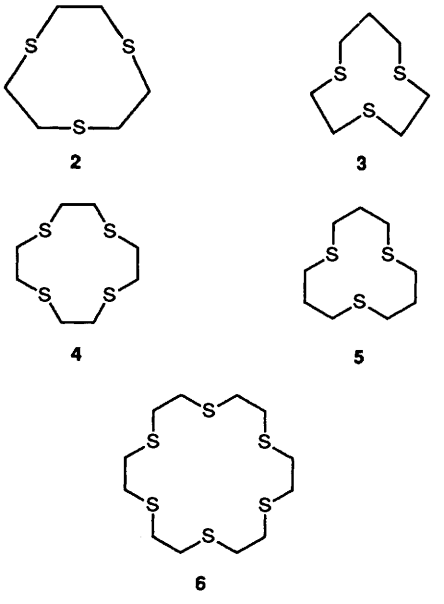

Experimental

Materials.—Commercially available thiocrowns **2**, **3**, **6** and deuteriated solvents were used (Aldrich).

NMR Data.—The ligands **2**, **3** and **6** were examined in $CDCl_3$ solution at 300 MHz (Bruker WB300) and/or 500 MHz (Bruker AMX500). The solutions were not degassed. Digital resolution was usually around 0.06–0.2 points Hz^{-1}. Line broadening of −0.5 Hz, and Gaussian broadening of 0.5 Hz were applied to enhance the apparent resolution. The S–C–C–S segments of **3**, which gave apparent AA′BB′ spectra were analysed with NUMARIT[8] to extract the average coupling constants for the segment, J, J' and J_{gem}. For **2** and **6**, the ^{13}C satellite signals in the proton spectra were obtained to allow sub-spectral analysis.[9] Derived coupling constants appear in Table 1, and calculated values in Tables 2 and 3.

Molecular Dynamics Procedure.—Crystal structures for **2** (the trithianonane),[6] **3** (the trithiodecane coordination complex[10]),

Table 1 Chemical shift and coupling constant data[a] for thiocrowns

Compound	δ_{obs}	$\frac{1}{2}J_{CH}$	J	J'	J_{gem}
1[b]	—	—	8.11(0.05)	2.40(0.05)	—
2	3.244	67.62	8.14(0.18)	2.51(0.18)	−13.03(0.13)
3	1.934, 2.071	—	7.96(0.10)	3.48(0.08)	−14.54(0.10)
6	2.785	70.15	9.72(0.04)	5.76(0.03)	−15.52(0.03)
7[c]	centred 2.9	—	9.1	6.1	−13.0
8[d]	—	—	8.1	2.79	—

[a] Shifts in ppm, J in Hz, solvent $CDCl_3$ unless stated otherwise: standard deviations in parentheses. [b] Data from ref. 17. [c] Data from ref. 20. [d] Data from ref. 21.

Table 2 Coupling constants calculated for the S–C–C–S segment in thiocrowns

Equation[a]	J(calc.)
$J_t^g = 1.35 + 0.63(E_x + E_y)$	4.63
$J_t^t = 18.07 - 0.88(E_x + E_y)$	13.49
$J_g^g = 8.94 - 0.94(E_x + E_y)$	4.05
$J_g^{g'} = 10.45 - 1.43(E_x + E_y)$	3.01
$J_g^t = 16.47 - 0.60(E_x + E_y)$	13.35

[a] From Abraham and Gatti, ref. 18.

Table 3 Averaged coupling constants calculated for the S–C–C–S segment in conformer mixtures

Ratio[a] $g_1:g_2:a$	J(calc.)/Hz	J'(calc.)/Hz	Comment
1:0:0	13.35	3.53	fixed *gauche* rotamer
1:1:0	8.18	3.79	all-*gauche* equilibrium
0:0:1	7.024	7.00	all-*anti* equilibrium
1:1:2	8.64	6.40	—
1:1:3	9.61	6.05	—
1:1:4	10.26	5.81	—
0:0:1	13.49	4.63	fixed *anti* rotamer

[a] Calculated for possible conformer mixes, assuming classical torsion angles for the S–C–C–S segment.

5, both as free ligand,[11] and as its ruthenium complex,[12] and **6** (the hexathiocyclooctadecane[13]) were used as starting points. Each molecule was assigned a type (thioether sulfur; SE; aliphatic carbon, CT; aliphatic hydrogen, HA) and a charge, using the molecular editor in QUANTA version 3.0 (QUANTA 3.0 by Polygen Corporation 1986, 1990). Charges were assigned using the charge templates option of the molecular editor within QUANTA. This method assigns charges from standard templates and gives charges consistent with the CHARMm forcefield. The charges are generally higher than when calculated using other methods (Gasteiger method, CNDO *etc.*). The structures were minimised using a value of 0.1 kcal mol^{-1} $Å^{-1}$ for the first derivative of the energy as the criterion for completion of minimisation. Version 21.2 of the commercial version of CHARMm[14] was used with the parameter file PARM30.PRM.

The following non-bonded parameters were used throughout.

```
INBFRQ 10 CUTNB 12.000000 CTONNB 10.500000 CTOFNB 11.00000 –
VSWITCH SHIFT RDIE EPS 1.000000
```

INBFRQ is the step frequency for updating the non-bonded list. CUTNB is the radius/Å beyond which non-bonded interactions are excluded in the list. VSWITCH and SHIFT refer to the smoothing functions used to avoid sharp non-bonded cutoffs, for van der Waals and electrostatics, respectively. CTONNB and CTOFNB are parameters to these functions, defining the range (radius/Å) over which they take effect. RDIE defines the distance-dependent dielectric. Electrostatic forces depend on the square of the inter-atomic distance. EPS is the value of the relative permittivity.

The following minimisation scheme was used:

```
MINI SD NSTEP 25
MINI ABNR NSTEP 150
MINI ABNR NSTEP 150
```

where NSTEP is the number of steps of minimisation, SD = Steepest Descents, a robust minimisation algorithm and ABNR = Adopted Basis-set Newton Raphson, a minimisation algorithm with better converging characteristics than steepest descents, although not so robust.

The molecules were all heated to 450 K over 9ps, equilibrated at this temperature for 10 ps and simulated for 610 ps. The temperature of 450 K was chosen after simulations at 300 K showed no signs of conformational change. Trials at higher temperatures indicated that this was as low a temperature as was consistent with conformational change within this timescale. The conformational transitions shown here might, therefore, be expected to occur at 300 K but with a longer life-time. Vacuum simulations were chosen in order to increase the accessible timescale. The general procedure follows. The time step is in picoseconds. Thus, "heat.inp" heats from 0.0 to 450 K over 9000 0.001 ps steps (*i.e.* 9 ps).

```
"heat.inp."
DYNA strt VERL –
TIME 0.001000 ISVFRQ 1000 IHTFRQ 200 IEQFRQ 0 IPRFRQ 1000 –
INBFRQ 10 CUTNB 12.000000 CTONNB 10.500000 CTOFNB 11.00000 –
VSWITCH SHIFT RDIE EPS 1.000000 –
NSTEP 9000 NSAVC 1000 NSAVV 1000 NPRINT 1000 –
FIRSTT 0.000000 FINALT 450.000000 – see below
TEMINC 10.000000 TWINDL – 10.000000 TWINDH 10.000000 –
ICHECW 1 –
IASORS 1 IASVEL 1 –
IUNREA –1 IUNWRI 31 KUNIT 34
"equil.inp"
DYNA rest VERL –
TIME 0.001000 ISVFRQ 1000 IHTFRQ 0 IEQFRQ 20 IPRFRQ 1000 –
NSTEP 10000 NSAVC 1000 NSAVV 1000 NPRINT 1000 –
FIRSTT 0.000000 FINALT 450.000000
"simul.inp"
DYNA rest VERL –
TIME 0.001000 ISVFRQ 1000 IHTFRQ 0 IEQFRQ 0 IPRFRQ 1000 –
NSTEP 610000 NSAVC 1000 NSAVV 1000 NPRINT 1000 –
FIRSTT 0.000000 FINALT 450.000000 –
IUNCRD 72 IUNVEL 73
```

Some variation of FINALT was necessary to stabilise the temperature at 450 K. The entire list of dynamics options is included only for heat.inp. For the other parts of the run only those options specific to equlibration/simulation etc. are included.

```
STRT/REST = start or restart simulation
VERL = the Verlet algorithm
```

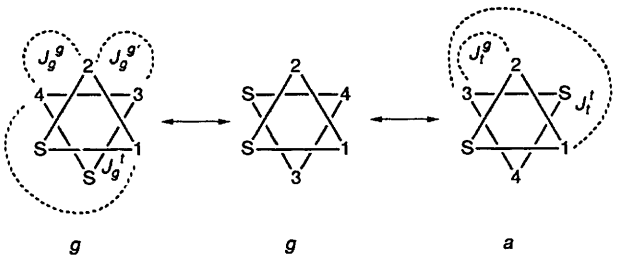

Fig. 1 This represents the geometrical relation of the H and S substituents on the SCH_2CH_2S fragment in the three perfectly staggered conformers. The coupling constants are show for each fixed conformer.

TIME = integration step in picoseconds
ISVFRQ = step frequency for updating the restart file
IHTFRQ = step frequency for increasing the temperature
IEQFRQ = step frequency for assigning or scaling velocities during equilibration
IPRFRQ = step frequency for printing averages and fluctuations of energies
NSAVC = frequency for saving coordinates
NSAVV = frequency for saving velocities
NPRINT = frequency for writing energies
FIRSTT = initial temperature in heating
TEMINC = temperature increment for heating every IHTFRQ step
TWINDL/TWINDH low and high deviations from the equilibration temperature above and below which velocities are assigned or scaled
ICHECW = if equal to 1 then velocities are assigned or scaled when the temperature falls outside the limits defined by TWINDL/TWINDH
If equal to 0 then no checking is performed
IASORS = option for either assigning (IASORS = 1) or scaling (IASORS = 0) velocities during equilibration
IASVEL = defines the method used for assigning velocities. In this case
IASVEL = 1. A Gaussian distribution of velocities is assigned
IUNREA/IUNWRI/KUNIT/IUNVEL/IUNCRD = fortran unit numbers for reading and writing the restart file and writing energies, coordinates and velocities
NSTEP = number of steps of dynamics
FINALT = temperature of equilibration/simulation

Note that these last two options needed to be varied for each molecule in order to simulate at 450 K. For the nonane **2** FINALT = 400 K, for the decane **3** FINALT = 450 K, for the dodecane **5** from the free structure FINALT = 450 K, for the built dodecane FINALT = 430 K, for the dodecane from the ruthenium complex FINALT = 430 K, and for **6**, the octadecane, FINALT = 450 K. During equilibration the temperature was unstable and so care was needed to ensure the simulation was running at the correct temperature.

Coordinates for the crystal structures used in the simulations were obtained from the CSSR files of the Chemical Databank at the SERC Daresbury facility, derived from the CDS system.[15]

Results and Discussion

Many crystal structures have been determined for thiocrowns. Although it has been customary in crown ether chemistry to consider conformations of the X–C–C–X unit, for thiocrowns with dimethylene links it is convenient to consider structures in terms of S–C–C–S–C–C–S, the so-called 'bracket' unit.[13] This is not present in either of the two simplest molecules, the 1,4-dithiane **1**, which occurs as a chair form (in the gas phase, as determined from electron diffracton data[16]), nor in the 1,4,7-trithiacyclononane **2**, which occurs with endodentate sulfurs in the highly symmetrical 333 conformation in the crystal,[6] and possibly in the same conformation or a 12222 conformation of C_1 symmetry in the gas-phase at *ca.* 500 K (as determined in a recent electron diffraction study[7]). The 1,4,7,10-tetrathiocrown-4 (**4**), may be regarded as the simplest molecule exhibiting two 'brackets,' fused at two sulfurs;[13] the hexathiocrown **6** crystallises[13] in a form with two brackets linked *via* C–C bridges. There is no structure for the free ligand **3**, 1,4,8-trithiocyclodecane, but there is a structure for a coordination complex[10] of **3**. The free ligand **5**, 1,5,9-trithiocyclododecane, forms what in projection looks like a square structure, reminiscent of other dodecane rings,[11] with one sulfur at a corner, but the other two in the middle of edges. Depending on the steric requirements of the metal, coordination complexes of these ligands have different geometries, in which as many sulfurs as required are placed *gauche* in order to interact with the metal ion. Coordination spheres may be completed by coordination with more than one ligand. Indeed, **5** forms a complex with copper in which its conformation scarcely differs from that in the free ligand, and only one of its sulfur atoms actually coordinates, that being exodentate;[11] its complex with Ru^{II} is a bis-(chelate).[12]

NMR Data.—Results of Lambert[17] on the simple system 1,4-dithiane **1** indicated that a *gauche* system (see Scheme 1),

1

Scheme 1

shuttling between two *gauche* forms, would give rise to the coupling constants observed. The equations derived empirically by Abraham and Gatti,[18] relating coupling constants for XCH_2CH_2Y protons (defined in Fig. 1) to electronegativities of the substituents X and Y, give rise to the values of J_t^g *etc.* shown in Table 2, corresponding to protons on SCH_2CH_2S segments, with classical torsion angles. Yet more sophisticated equations are available,[19] but their application demands a knowledge of the angles of the fragment of interest, and these will not be considered here. It can be seen that a pure *anti* (*gauche*) conformation would give $J_t^t(J_g^t)$ around 13.49 (13.35) with $J_t^g(J_g^g)$ near to 4.63 (3.01). Assembled in Table 3 is a set of averaged coupling constants, based on the values in Table 2, and calculated for particular conformational mixes. These should be compared with the experimental values in Table 1.

The values observed for the dithiane are close to those expected for two *gauche* conformations in rapid equilibrium. Using the same technique (^{13}C satellite spectra[9]), we have determined that the coupling constants for the nonane **2** are almost identical to those of the dithiane, and concluded that **2** is fluxional between *gauche* conformers, with little evidence of any *anti* conformers. The photoelectron spectroscopic studies of Glass *et al.*[20] suggest a 333 geometry, since the observed energy levels are consistent with those obtained from a MINDO/3 (full geometry optimised) calculation: the more recent gas phase electron diffraction study of Blom *et al.*[7] is also instructive, since the observed diffraction pattern although possibly consistent with a 333 structure, fits better to a C_1 structure (which also gave the lowest MM2 energy of the set of conformers considered). The overall interpretation of Blom *et al.* did not discount a mixture of possible conformers, which conceivably could also fit the experimental diffraction data.

The results for **3** indicate that the ligand is fluxional, but the coupling constants for the 'averaged' AA′BB′ segment may be extracted. These are considerably divergent from the estimated

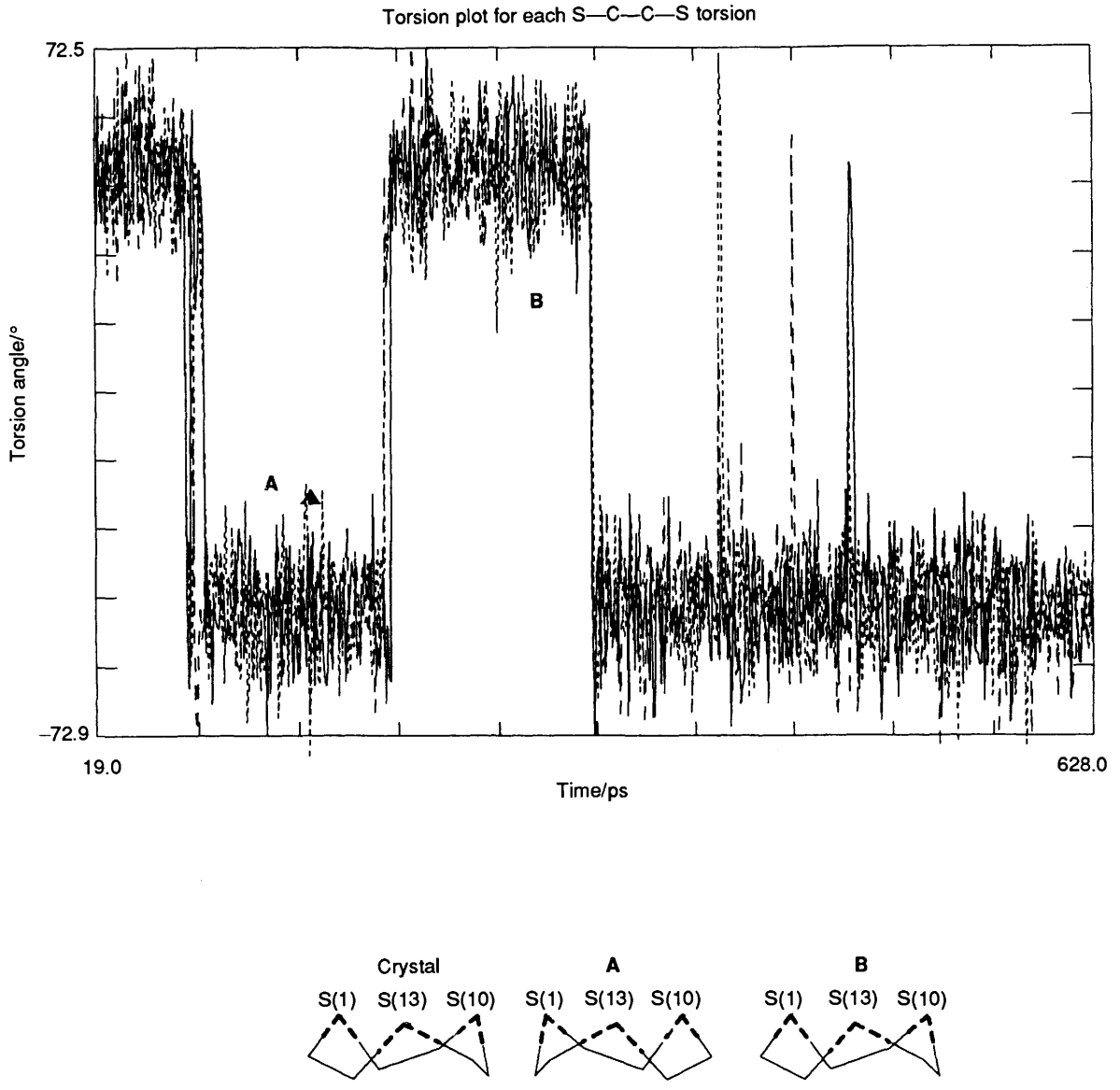

Fig. 2 Dynamic analysis of the trithianonane **2** from the crystal structure conformation. The trace shows the close similarity in the development of each of the C–C torsions during the run. Below are depicted the two minimised average structures labelled A and B, corresponding to the metastable sections of the trace used for the average, indicated as A and B, and the crystal structure (miminised).

coupling constants (Table 2) for either *gauche* or *anti* segments, but permit the same interpretation as for the nonane, with an equilibrium between *gauche* conformers (see Table 3). A germocane **8** containing the S–C–C–S–C–C–S unit, and whose

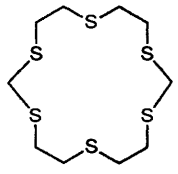

7

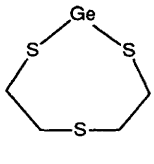

8

crystal structure[21] indicates *gauche* torsion angles for the S–C–C–S units, has similar coupling constants. This eight-membered ring is also proposed to be in a rapid equilibrium of *gauche* conformers in solution.

A distinctive range of coupling constants (9.72 and 5.76) is obtained from the ^{13}C satellites of the ^{1}H NMR spectrum of hexathiocyclooctadecane **6**; these clearly are an average, indicative of a mixture of *gauche* and *anti* segments with a high proportion of *anti*, based on the estimate of the averaged J to be expected for a particular mixture of conformers. The coupling constants reported for the sixteen-membered ring[22] **7** again are very similar, and may be interpreted with reference to Table 3. An analysis of the exact proportions of conformers depends on knowing the exact values of the coupling constants in a rigid segment. However, the MD results indicate the futility of interpreting the coupling constants in more detail, since the conformational equilibria are extremely complex.

Molecular Dynamics Results.—The thiocrowns were also simulated using molecular dynamics methods. It was necessary first to determine a realistic protocol, which could be applied to each of the ligands in a closely similar way, so that the results would be comparable. This is discussed in the Experimental section on MD. It was hoped to probe the nature of the individual conformations in the mix from a sufficiently extended simulation. Thus the behaviour was scanned using torsion angles of the S–C–C–S segments (or, for ligands **3** and **5**, a C–C–C–S segment) as marker. Plots of the chosen torsion(s) *versus* time are shown for each of the compounds **2**, **3**, **5** and **6** (Figs. 2–7) and each is discussed in turn, highlighting the results of

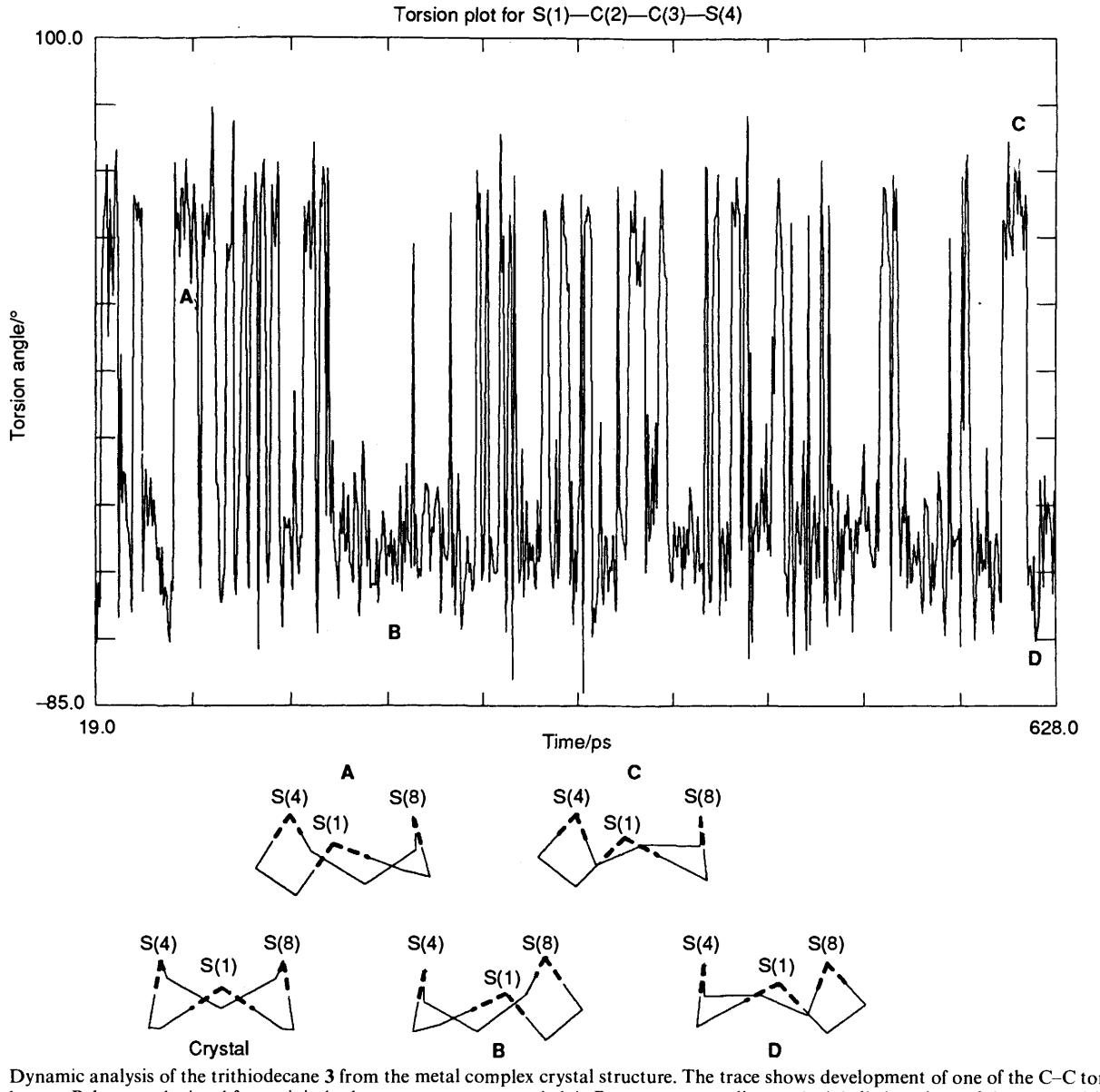

Fig. 3 Dynamic analysis of the trithiodecane **3** from the metal complex crystal structure. The trace shows development of one of the C–C torsions during the run. Below are depicted four minimised average structures coded A, B, *etc.* corresponding to the labelled sections of the run used for the average, plus the (minimised) crystal structure.

relevance to the conformational study. Tabulated data relating to the torsion angles of all the derived structures (A, B, C *etc.* in Figs. 2–7) are given as Supplementary Data [sup. no. 56872 (7 pp.)].* The statistics relating to each run are gathered in Table 4. The simulations were carried out for a total of 600–1800 ps. During this time, transitions between torsional potential wells, corresponding to conformational switches of the individual torsion angles are to be expected,[2,3] on timescales of 10 ps upwards, while small-amplitude oscillations within a potential well are expected on a sub-picosecond timescale. The natural interpretation of the simulations is that the large variations seen correspond to changes of the chosen torsion from one torsional minimum to another. Table 5 indicates the part of the simulations from which averaged structures were prepared. Since the molecules are all complex, the results for one torsion alone are not very informative about the rest of the molecule. Thus a display of the averaged (and then minimised) structure for each metastable section of the trace is shown. This is a particularly economical and informative way of representing the very complicated results of an MD simulation.

Nonane **2**.—The results for this ligand are the simplest and the easiest to interpret. The three traces (which almost superpose) shown in Fig. 2 show the time-evolution of each of the three C–C torsion angles undergoing g^+–g^- transitions. The movement of each of the three torsions is correlated. Each metastable section corresponds to all-*gauche* structures with either all-plus or all-minus torsion angles. The averaged structure of each section was minimised (details are shown in Fig. 2 and Table 5). One conformation, B, is identical to the crystal structure; while A is identical to the mirror image. A superposition of the whole set of structures corresponding to A, together with those corresponding to B is displayed in Fig. 8. Each structure was fitted (least squares) to the final structure to fix each structure in space. One is clearly the mirror image of the other. This representation makes abundantly clear the multiplicity of structures available at this temperature. The first section of Fig. 2, including a transition from + to − of the C–C torsions, at *ca.* 71.55 – 85.05 ps was examined in more detail.

* For details of the Supplementary Data scheme, see 'Instructions for Authors' (1992), *J. Chem. Soc., Perkin Trans. 2*, in the January issue.

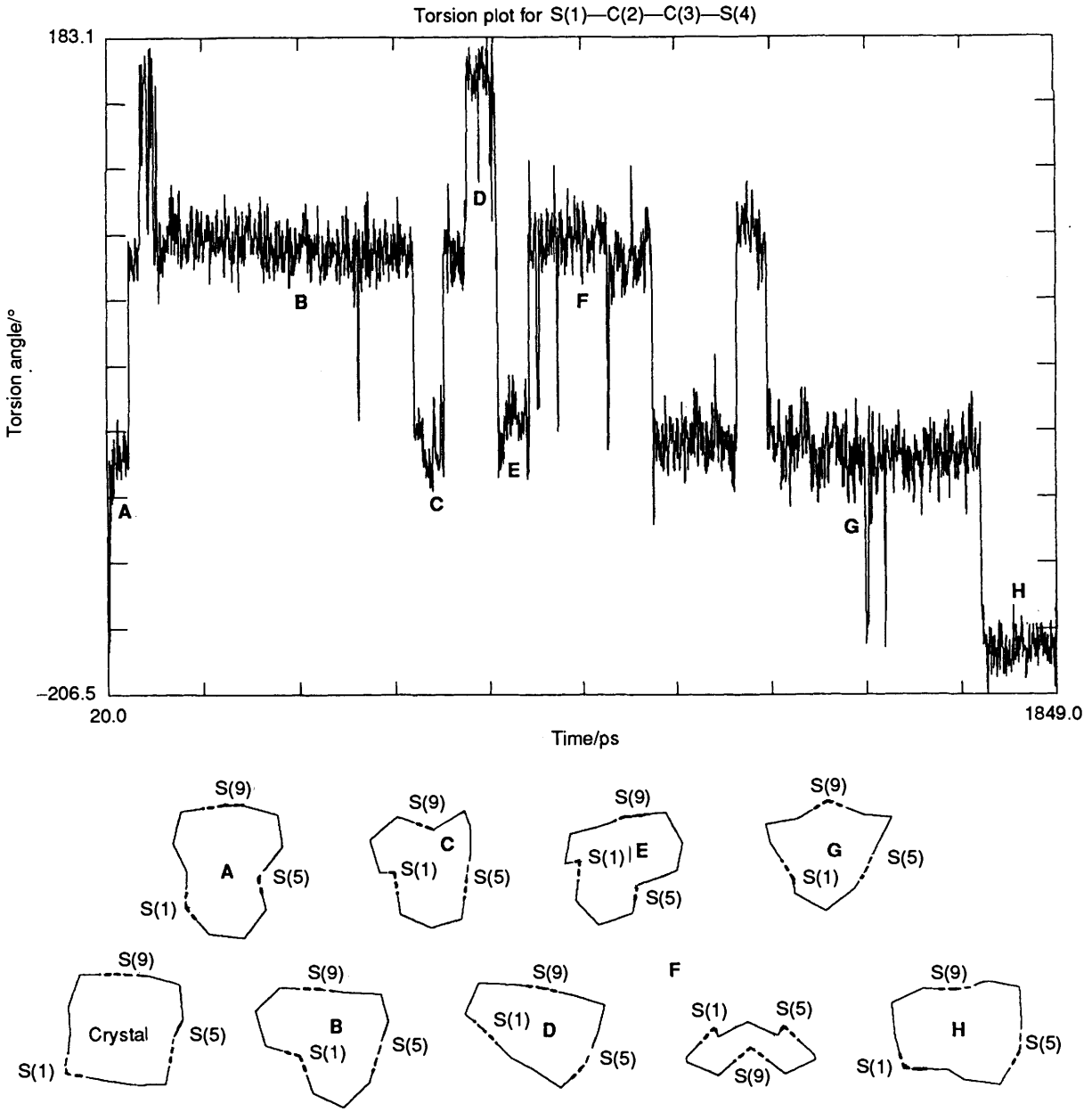

Fig. 4 Dynamic analysis of the trithiododecane **5** from the crystal structure of the free ligand. The trace shows development of one of the C–C torsions during the run. Below are eight minimised averaged structures coded A, B, C, *etc.* corresponding to the labelled sections of the run used for the average, together with the minimised crystal structure.

Table 4 Statistics for molecular dynamics simulations

	Mean energy[a]			
Compound	Total energy	Kinetic energy	Potential energy	Mean temperature[a]
2	60.16 (0.12)	24.93 (3.38)	35.24 (3.45)	440.11 (59.59)
3	71.16 (0.15)	30.35 (3.67)	40.81 (3.76)	462.87 (55.99)
5 free	83.13 (0.16)	37.69 (4.14)	45.43 (4.24)	451.61 (49.65)
5 built	84.16 (0.17)	37.48 (4.19)	46.68 (4.29)	449.01 (50.25)
5 metal	84.31 (0.17)	38.17 (4.31)	46.14 (4.42)	457.38 (51.69)
6	115.24 (0.19)	53.72 (4.93)	61.52 (5.03)	450.58 (41.31)

[a] In kcal mol^{-1}. Standard deviation in parentheses. [b] In K. Standard deviation in parentheses.

This is shown in Fig. 9, in which every fiftieth structure from the simulation is represented.

The ground-state structure of this crown, with its three-fold symmetry, is reminiscent of a three-bladed propeller, if the 'hub' is considered to be the empty space at the centre of the molecule, and the three 'blades' are thought to be the S–C–C–S segments. Thus the molecule may have a right-handed screw, and a left-handed screw, as shown in Fig. 8. Correlated movement of the rings in a triaryl propeller has been demonstrated and attempts have been made to rationalise the reaction pathway in terms of

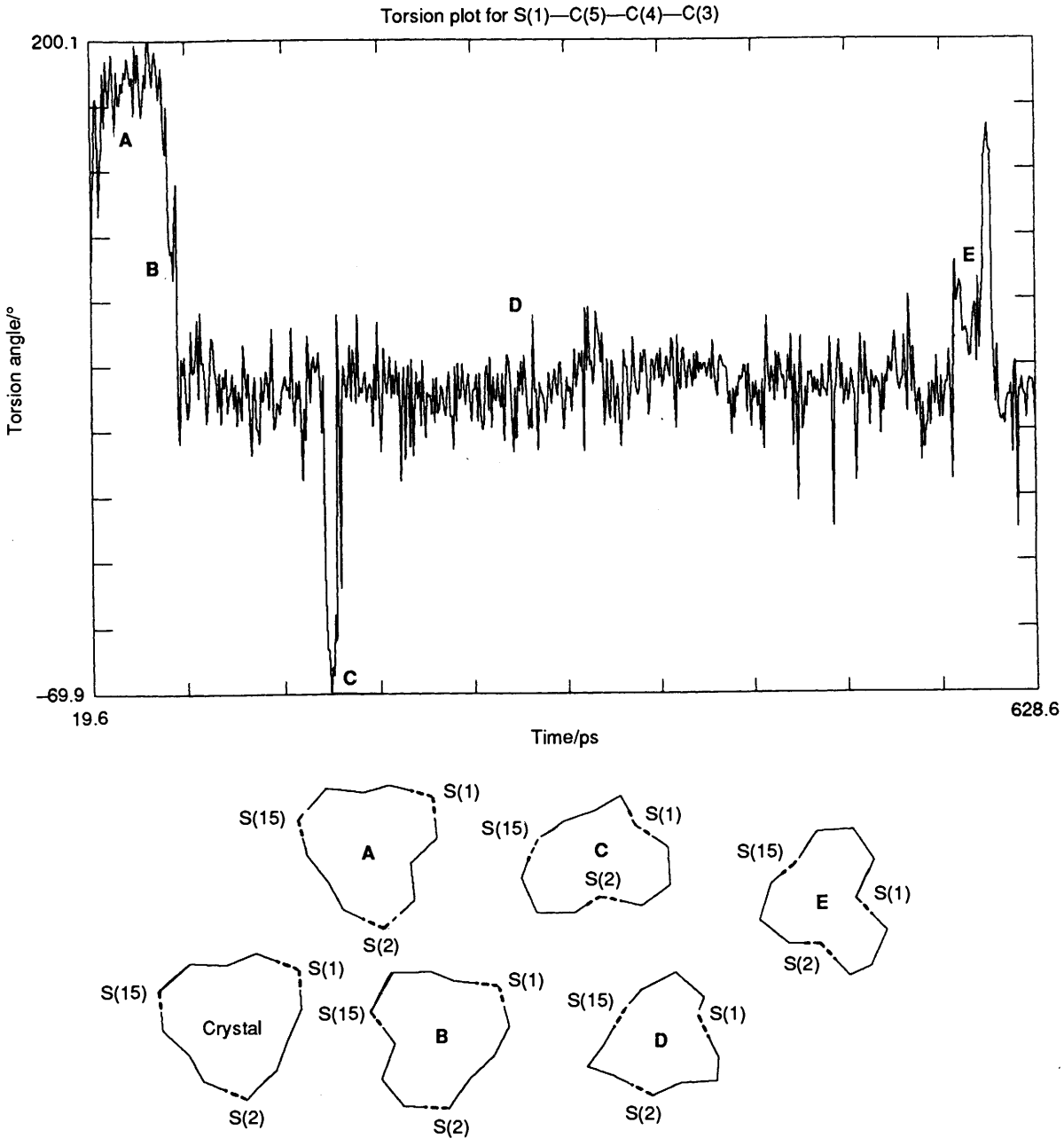

Fig. 5 Dynamic analysis of the trithiododecane **5** from a built structure. The trace shows development of one of the C–C torsion angles during the run. Below are five minimised average structures coded A, B, C, *etc.* corresponding to the labelled sections of the run used for the average, plus the minimised crystal structure.

Table 5 Sections of the simulations sampled for the average structures [a]

	A	B	C	D	E	F	G	H
2	85–195	200–320	—	—	—	—	—	—
3	70–79	194–212	595–606	611–617	—	—	—	—
5 free	30–62	120–600	630–662	713–756	770–828	830–1070	1300–1700	1710–1849
5 built	27–70	70–75	168–175	190–570	577–602	—	—	—
5 metal	45–145	216–230	240–628.6	950–1180	1239.6–1267	1420–1660	1730–1848.6	—
6	61–75	91–112	189–230	248–262	266–288	387–409	416–421	467–485

[a] In picoseconds.

the individual movement of the aryl rings relative to a defined molecular plane.[24]

Pursuing this analogy, one may look for relative movements of the three segments of the thiocrown in the small section of the trace which has been expanded in Fig. 9. The first torsional barrier crossing in the pathway indicates several approaches of the molecule to the barrier; one torsion moves through zero first, followed in 10 fs by the second; this after 100 fs reverses, followed by movement of the third torsion, reversal of the first, then after *ca.* 200 fs the first angle flips rapidly three times, accompanied by the flip of the second angle: the molecule then settles down into the new metastable conformation. This

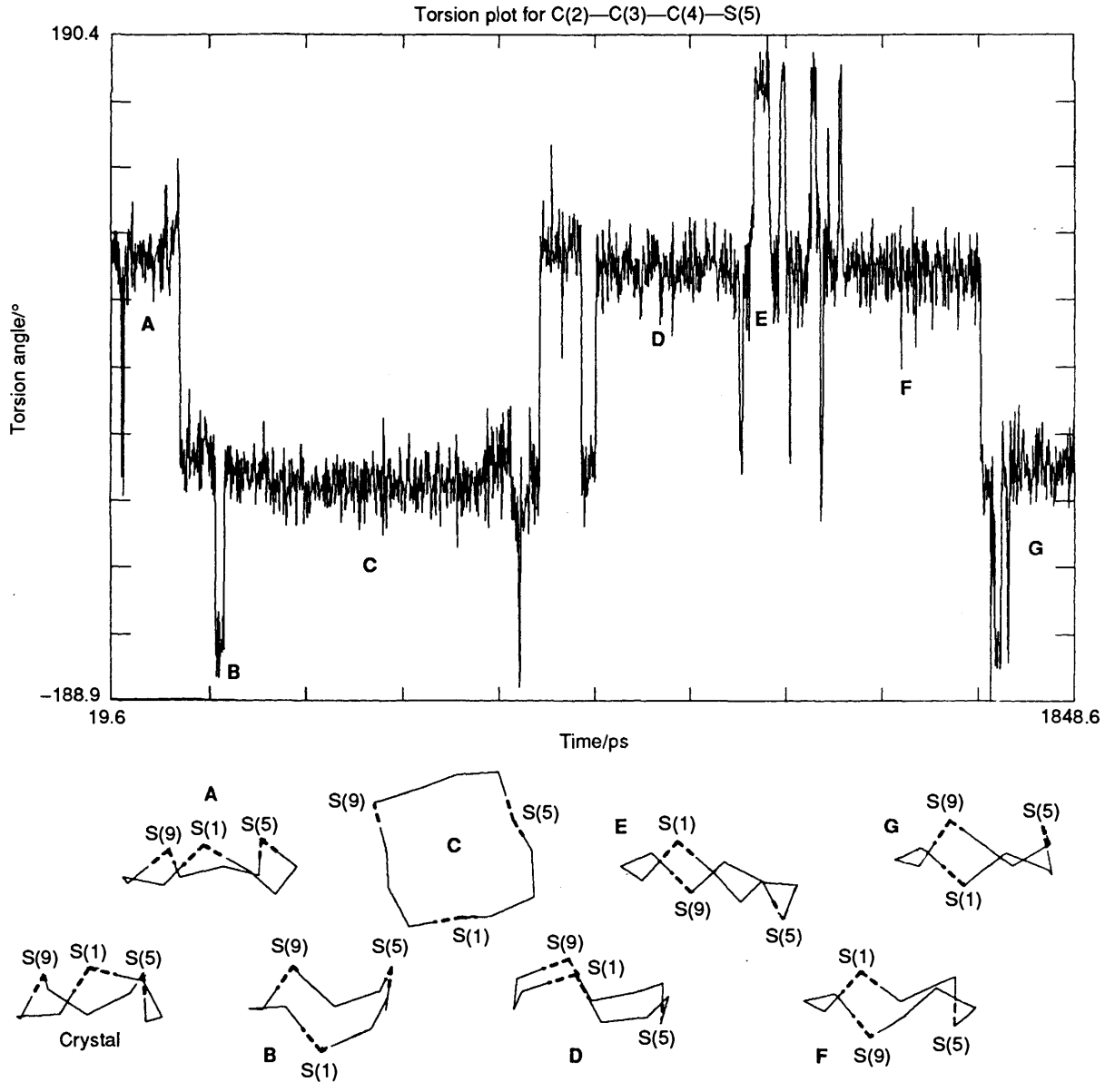

Fig. 6 Dynamic analysis of the trithiododecane **5** from the ruthenium complex crystal structure. The trace shows the development of one of the C–C torsions during the run. Below are seven minimised average structures coded A, B, C, *etc.* corresponding to the labelled sections of the run used for the average, plus the minimised crystal structure.

suggests that each torsion moves independently, but that the first movement initiates a train which leads to the complete surmounting of the barrier, when the 'propeller' switches pitch. The torsional movement is through an S–C–C–S torsion angle of zero. It seems entirely reasonable that only one such torsional change could occur at a time.

Decane **3**.—The trace (Fig. 3) shows one of the S–C–C–S torsions and one of the S–C–C–C torsions. *gauche–gauche* transitions are seen for both torsions and four structures are shown. As with the nonane, mirror image conformations are seen (**A**–**B** and **C**–**D**). The S–C–C–S units are both *gauche* throughout the simulation time shown on the trace and the sulfurs present an endodentate conformation. The average of the **A** and **B** structures is similar to the crystal structure. It is obvious that the simulation never reproduces the crystal structure. However, this was taken from a metal complex and is presumably stabilised only in the presence of the metal ion.

Dodecane **5**.—The traces in Figs. 4–6 show torsion angle plots for the dodecane starting from (*a*) the crystal structure of the free ligand, (*b*) the structure built from scratch and (*c*) the ligand from the crystal structure of the ruthenium complex, respectively. Structures for the parts of the simulation indicated were taken and compared. Whereas the crystal structure for the free ligand shows the characteristic square-bracket conformation of the thiocrowns, this is seen again only in structure **H**. For the rest of this simulation, if we consider the way in which the sulfur atoms point towards the ligand face (taken as up or down), various 2-up, 1-down (1-up, 2-down) endodentate structures are seen. One 3-up, endodentate structure, similar to the metal complex crystal structure was found (structure **F**). For the simulation initiated from the built structure, although the initial structure is very different from the free crystal structure, both structures **A** and **B** have the characteristic exodentate bracket of the free crystal structure. Once again, we also see various 2-up, 1-down structures. For the simulation initiated from the crystal structure of the ruthenium complex, the 3-up structure disappears after *ca.* 100 ps of simulation. For the rest of the time, 2-up, 1-down structures predominate except for structure **C**, which is identical to the free crystal structure.

For each of these three simulations, it is notable that the

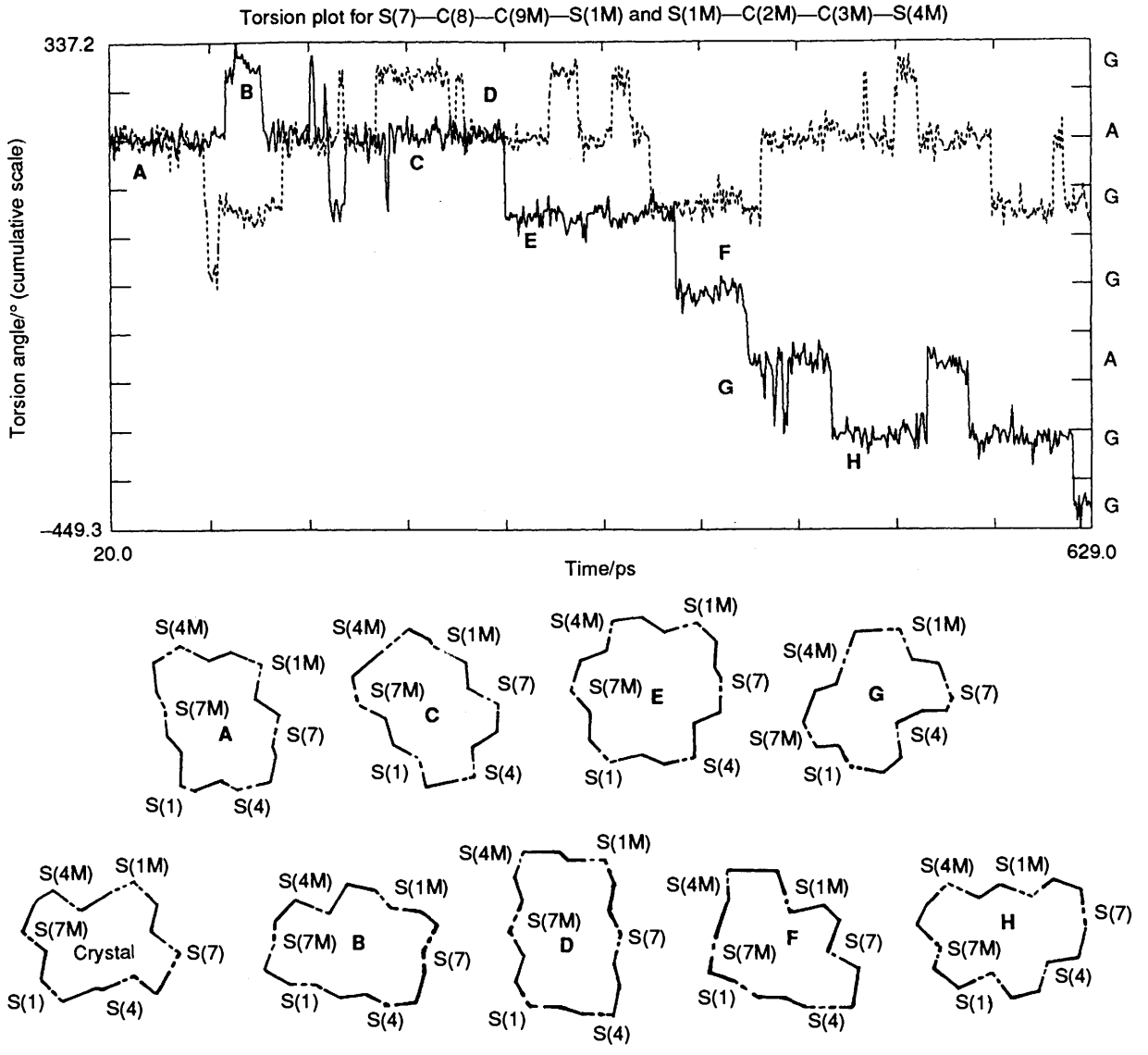

Fig. 7 Dynamic analysis of the hexathiocrown **6** from the crystal structure. The trace shows the development of two of the C–C torsions during the run. An indication is given on the right of the plot of *gauche* (G) or *anti* (A) torsion angle. Below are eight minimised average structures, coded A, B, C, *etc.* corresponding to the labelled sections of the trace used for the average, plus the minimised crystal structure.

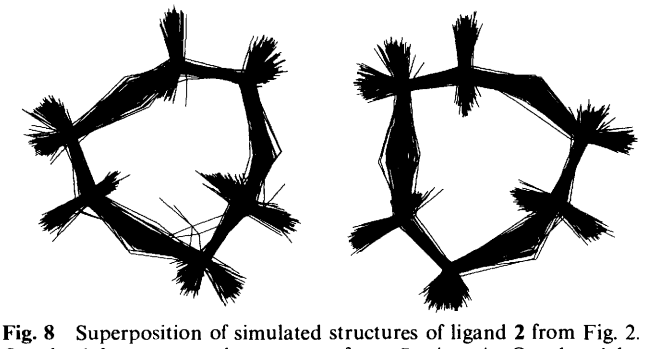

Fig. 8 Superposition of simulated structures of ligand **2** from Fig. 2. On the left, superposed structures from Section A. On the right, superposed structures from Section B.

S–C–C–C torsions which develop are essentially all *gauche*—only 7% were *anti* if the first section of the trace from the scratch structure is ignored, and in only one of the structures (C, derived from the Ru complex) are there two *anti* torsions in the one structure, as found in the free ligand.

Hexathiocrown **6**.—This shows greater flexibility than do **2**, **5**, as seen from the torsion angle scale (Fig. 7). The C–C torsions are able to undergo complete 360° spins. The bracket structure seen in the crystal, reappears in structures C and D, but the other structures are quite different. These structures were picked to provide a good selection of values for three of the six C–C torsions. Obviously, other structures exist which are not represented here. However, the proportion of *anti* torsions is about equal to the proportion of *gauche* summed over the selected metastables. The metastable sections corresponding to an *anti* angle for the chosen segment occupy *ca.* 50% of the trace, with *gauche* conformers occupying the other 50%. Also evident is the greater tendency for *anti–gauche* rather than *gauche–gauche* flips for the two torsions which were scanned. This is consistent with the zero torsion angle (eclipsed sulfurs) being less favourable than the 120° angle (eclipsed hydrogens, or hydrogen/sulfur). The present study is insufficiently detailed to indicate if the torsional switching in the hexacrown is correlated or not.

General Inferences.—The nonane **2** is the least flexible, permitting essentially a *gauche–gauche* switch, and on a relatively long timescale (*ca.* 60–100 ps) compared to the switches observed with the other systems studied. The hexathiocrown **6**, on

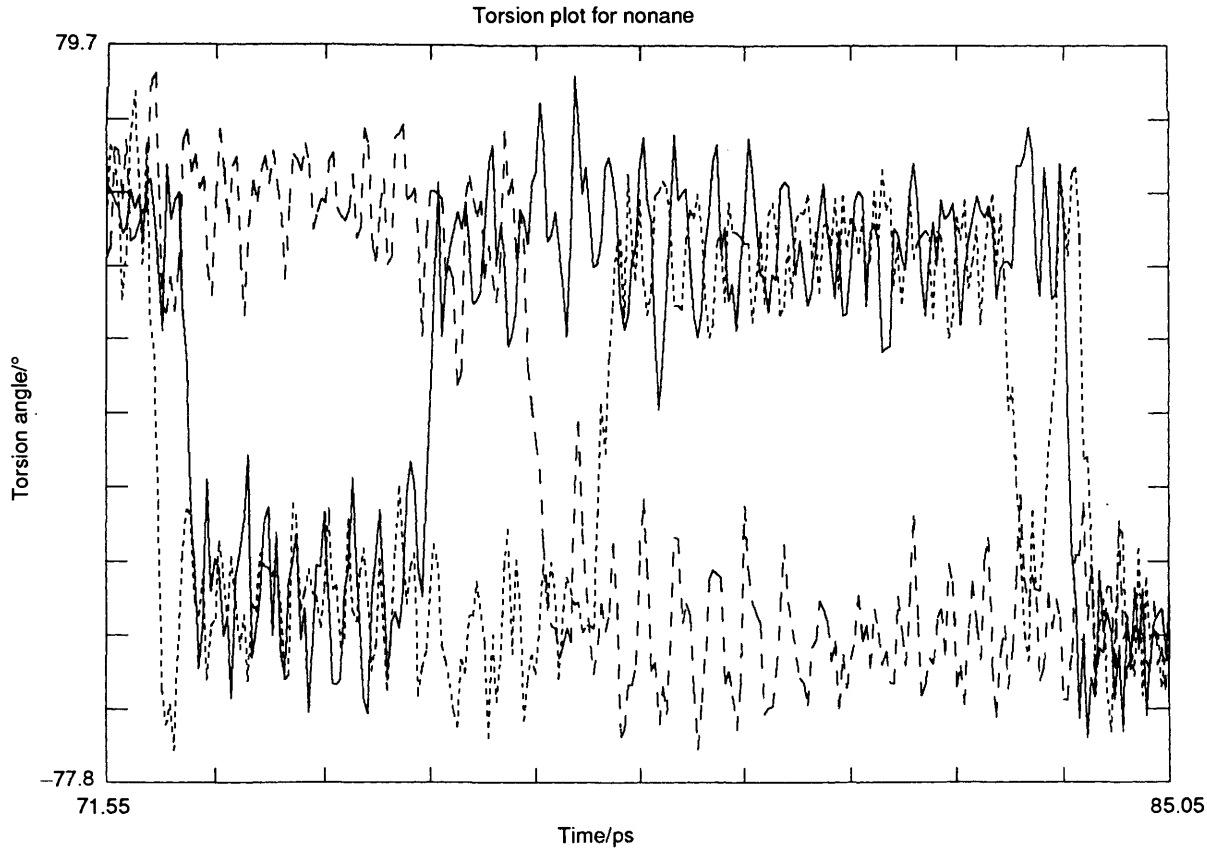

Fig. 9 Expansion of the section of Fig. 2 corresponding to a transition from + to − of the C–C torsions of ligand **2**

Table 6 Conformation process noted

Ligand	NMR	MD	Torsional timescale/ps
2	$g \rightleftharpoons g$	$g \rightleftharpoons g$	*ca.* 100
3	$g \rightleftharpoons g$	$g \rightleftharpoons g$	*ca.* 10
5	—	all g	100–200
6	$g \rightleftharpoons t$	$g \rightleftharpoons t$	10–30
	$g \rightleftharpoons g$	$g \rightleftharpoons g$	—

the other hand, is much more flexible, and a full range of torsion angles is open to each segment. While the simulations started from the free ligand crystal structures appear to provide confirmation of the general prejudice that the structure is perpetuated on average in solution, the results from the three different starting points for the dodecane give a warning, that the protocol adopted may not be sufficient to enable the full conformational surface to be sampled even within this timescale, and at the temperature used, especially for a structure built from scratch.

Conclusions

Interpretation of both the experimental (NMR) and theoretical (MD) results, has indicated the general nature of the conformational mix obtained. It is encouraging that for thiocrowns **2**, **3** and **6**, for which the results from the two different approaches may be compared, the indications are qualitatively similar (see Table 6). Several recent studies have attempted to use molecular mechanics calculations in the interpretation of NMR spectra. For example, Son *et al.*[25] have used MM2 calculations to generate a range of possible conformers, estimated their respective MM energies, and then calculated the population of each to be expected on the basis of the Boltzmann distribution. Individual J values were then weighted in a Boltzmann relation. With MD techniques, one can sample conformational space, on timescales sufficient to sample shape changes, and the accessible structures are more likely to be representative of the real situation. Although one could extract many structures from each trajectory, nevertheless the calculation and weighting of J values for each of these would be an exceptionally long task, and has not been attempted here. Such calculations might in future be incorporated as a module in the modelling software. However, the results of this study emphasise the futility of operating on a few ground state structures (from MM studies) to calculate solution properties, when the true situation is of an enormous number of structures, each with a considerable population. In future work we hope to tackle the effects of metal ion coordination on the dynamics.

Acknowledgements

The authors thank the SERC for financial support, Mr. G. Smiley for some preliminary work and Dr. M. N. S. Hill and Professor W. MacFarlane for the NMR spectra.

References

1 J. C. Lockhart, M. B. McDonnell, M. N. S. Hill, M. Todd, *J. Chem. Soc., Perkin Trans. 2*, 1989, 1915.
2 S. R. Cooper and S. C. Rawle, *Structure and Bonding*, Springer-Verlag, Berlin, 1990, **72**, 1.
3 A. J. Blake and M. Schroeder, *Adv. Inorg. Chem.*, 1990, **35**, 1.
4 D. J. Cram, *Angew. Chem., Int. Ed. Engl.*, 1986, **25**, 1039.
5 T. W. Bell, F. Guzzo and M. G. B. Drew, *J. Am. Chem. Soc.*, 1991, **113**, 3115.
6 R. S. Glass, G. S. Wilson and W. N. Setzer, *J. Am. Chem. Soc.*, 1980, **102**, 5068.
7 R. Blom, D. W. H. Rankin, H. E. Robertson, M. Schroeder and A. Taylor, *J. Chem. Soc., Perkin Trans. 2*, 1991, 773.
8 NUMARIT, J. S. Martin and A. R. Quirt, *J. Magn. Reson.*, 1971, **5**, 318; version provided by the SERC NMR Program Library, 1981.

9 N. Sheppard and J. J. Turner, *Proc. R. Soc. London, Ser. A*, 252, 506; R. J. Abraham, *Analysis of High Resolution NMR Spectra*, Elsevier, Amsterdam, 1971.
10 W. N. Setzer, E. L. Cacioppo, Q. Guo, G. J. Grant, D. D. Kim, J. L. Hubbard and D. G. VanDerveer, *Inorg. Chem.*, 1990, **29**, 2672.
11 S. C. Rawle, G. A. Admans and S. R. Cooper, *J. Chem. Soc., Dalton Trans.*, 1988, 93.
12 S. C. Rawle, T. J. Sewell and S. R. Cooper, *Inorg. Chem.*, 1987, **26**, 3769.
13 R. E. Wolf, J. R. Hartman, J. M. E. Storey, Bruce M. Foxman and S. R. Cooper, *J. Am. Chem. Soc.*, 1987, **109**, 4328.
14 B. R. Brooks, R. E. Bruccoleri, B. D. Olafson, D. J. States, S. Swaminathan and M. Karplus, *J. Comput. Chem.*, 1983, **4**, 187.
15 F. H. Allen, O. Kennard and R. Taylor, *Acc. Chem. Res.*, 1983, **16**, 146.
16 O. Hassel and H. Viervoll, *Acta Chem. Scand.*, 1947, **1**, 149.
17 J. B. Lambert, *J. Am. Chem. Soc.*, 1967, **89**, 1836.
18 R. J. Abraham and G. Gatti, *J. Chem. Soc., B* 1969, 961; R. J. Abraham, C. J. Medforth and P. E. Smith, *J. Comp.-Aided Mol. Design*, 1991, **5**, 205.
19 C. A. G. Hasnoot, F. A. A. M. De Leuuw and C. Altona, *Tetrahedron*, 1980, **36**, 2783.
20 W. N. Setzer, B. R. Coleman, G. S. Wilson and R. S. Glass, *Tetrahedron*, 1981, **37**, 2743.
21 M. Drager, *Chem. Ber.*, 1975, **108**, 1723; M. Drager and L. Roos, *Chem. Ber.*, 1975, **108**, 1712.
22 B. de Groot and S. J. Loeb, *Inorg. Chem.*, 1989, **28**, 3573.
23 R. M. Levy, M. Karplus and P. G. Wolynes, *J. Am. Chem. Soc.*, 1981, **103**, 5998.
24 W. Clegg and J. C. Lockhart, *J. Chem. Soc., Perkin Trans. 2*, 1987, 1621.
25 P. S. Son, T.-Y. Lin, T. Grzybowski, N. H. Cromwell and C. A. Kingsbury, *J. Chem. Soc., Perkin Trans. 2*, 1991, 313.

Paper 1/04540G
Received 2nd *September* 1991
Accepted 17th *December* 1991